Hereditary Spherocytosis Caused by a Novel Compound Heterozygous Mutation of the *SPTA1* Gene and Autoimmune Hepatitis in a Pediatric Patient

Yu-mei Qin
Guangxi Medical University First Affiliated Hospital
Yan-yun Chen
Guangxi Medical University First Affiliated Hospital
Lin Liao
Guangxi Medical University First Affiliated Hospital
Yang-yang Wu
Guangxi Medical University First Affiliated Hospital
Min Chen
Guangxi Medical University First Affiliated Hospital
Fa-quan Lin (faquanlin@163.com)
Guangxi Medical University First Affiliated Hospital https://orcid.org/0000-0002-8631-4339

Research article

Keywords: Autoimmune hepatitis, Hereditary spherocytosis, Alpha-spectrin, DNA mutational analysis, Diagnosis

Posted Date: November 1st, 2021

DOI: https://doi.org/10.21203/rs.3.rs-1023423/v1

Abstract

Objective: Patients suffering from both hereditary spherocytosis (HS) and autoimmune hepatitis (AIH) are very rare. We analyzed the clinical and genetic characteristics of a seven-year-old girl with yellow sclerae and abnormal liver function tests, but no further symptoms.

Methods: Blood samples were collected from the proband, her parents, and her paternal grandmother, and analyzed using routine laboratory tests, as well as subjected to next-generation and Sanger sequencing.

Results: Compound heterozygous mutations of the spectrin alpha, erythrocytic 1 (*SPTA1*) gene were identified in the proband. Thec.134G>A (p.R45K) and c.6544G>C (p.D2182H) mutations were inherited from her mother and father, respectively. The proband's father and paternal grandmother had the same mutation. Neither mutation is described in the Human Gene Mutation Database.

Conclusions: HS has clinical manifestations similar to AIH, it may be difficult to diagnose when it coexists with AIH. When laboratory results cannot be explained by autoimmune liver disease alone, the possibility of a concomitant disease should be considered. Pedigree investigation and genetic analyses might be required to arrive at the final diagnosis.

1. Introduction

Autoimmune hepatitis (AIH)[1] is a chronic inflammatory liver disease characterized by an autoimmune response in liver cells that may lead to cirrhosis and liver failure [1]. AIH occurs worldwide. A national epidemiological survey in Finland showed that the incidence of AIH was 14.3 per 100,000 in 2019, with an increasing trend thereafter [2]. In the United States, the incidence of AIH was approximately 31.2 per 100,000 between 2014 and 2019 [3].

Hereditary spherocytosis (HS) is a common familial hemolytic disorder caused by mutations in genes encoding erythrocyte membrane proteins; most of the mutations are autosomal dominant, but a few are autosomal recessive [4]. Typical clinical symptoms of patients with HS include anemia, jaundice, and splenomegaly [5]. Like, AIH, HS is observed globally. In the Nordic region, the incidence of HS was as high as 1/2000 [6], and the prevalence in China was reported to be about 1 in 100,000 people [7].

To date, pathogenic variants of the genes *ANK1*, *SPTB*, *SPTA1*, *SLC4A1*, and *EPB42* that encode the erythrocyte membrane proteins ankyrin, β-spectrin, α-spectrin, band 3 protein, and 4.2 protein, respectively, have been related to HS [8]. Patients with both HS and AIH have not been reported in China. Herein, we describe a seven-year-old girl with HS occurring concomitantly with AIH, who was admitted to the First Affiliated Hospital of Guangxi Medical University in Guangxi, China. To improve the clinical understanding of this rare condition, we analyzed the clinical characteristics of HS and AIH in the patient and genetically analyzed the patient, her parents, and her paternal grandmother.

[1]AIH, autoimmune hepatitis; ALT, alanine aminotransferase; ANA, antinuclear antibody; AST, aspartate aminotransferase; DBIL, direct bilirubin; G6PD, glucose-6-phosphate dehydrogenase; Hb, hemoglobin; HS, hereditary spherocytosis; IBIL, indirect bilirubin; Ig, immunoglobulin; MCHC, mean corpuscular hemoglobin concentration; MCV, mean corpuscular volume; MSCV, mean sphered corpuscular volume; MRV, mean reticulocyte volume; NGS, next-generation sequencing; RBC, red blood cell count; RET, reticulocyte count; SMA, anti-smooth muscle antibody; TBIL, total bilirubin

2. Material And Methods

2.1 Clinical history

The patient was a girl born in Guangxi Zhuang Autonomous Region of China in June 2014. At the age of four years, she was admitted to our hospital with “sclera yellowing for more than four months, and liver function damage for four days.” In April 2017, during her physical examination for kindergarten admission, the child was found to have yellowish sclerae and slightly increased levels of transaminases and bilirubin. The yellow tinge of her sclerae subsequently resolved spontaneously. Four months later, the child developed yellowish sclerae again, and her transaminase and bilirubin serum levels were three times higher than the normal range. She was diagnosed with liver damage in another hospital and received liver protection treatment for two days. The yellow scleral color resolved, and the patient was transferred to our hospital for further diagnosis and treatment. Physical examination showed yellowish sclerae, no obvious anemia, no lymph-node enlargement, and normal auscultation of both lungs. However, her liver was palpable 4 cm below the xiphoid process, and the spleen could be felt 3 cm caudally of the lower ribs. Laboratory test results showed a red blood cell count (RBC) of 3.93×10^{12}/L, hemoglobin (Hb) of 114.7 g/L, reticulocyte percentage (RET) of 10.3 %, mean corpuscular hemoglobin concentration (MCHC) of 359.10 g/L, mean corpuscular volume (MCV) of 81.35 fL mean sphered corpuscular volume (MSCV) of 60.29 fL, and mean reticulocyte volume (MRV) of 73.04 fL. Spherical cells accounted for 18 % of the red blood cells in peripheral blood smears. A thalassemia gene test showed no abnormality, glucose-6-phosphate dehydrogenase (G6PD) activity was normal, and the Coombs test was negative. Liver function tests showed the following serum levels: total bilirubin (TBIL) 64.30 μmol/L, direct bilirubin (DBIL) 32.00 μmol/L, indirect bilirubin (IBIL) 32.30 μmol/L, alanine aminotransferase (ALT) 137 U/L, and aspartate aminotransferase (AST) 107 U/L (Table 1). An investigation of autoantibodies associated with autoimmune liver disease showed weakly positive results for antinuclear antibodies (ANAs). Immunofluorescence staining demonstrated that the ANA karyotype (1:100) was homogeneous. Anti-smooth muscle antibodies (SMAs) were positive with a titer of 1:320. Serum protein electrophoresis showed increased γ-globulins; immunoglobulin (Ig)G was elevated to 18.89 g/L. All tests for hepatotropic viruses were negative. Levels of blood copper and ceruloplasmin and urine copper were normal. Histological examination of the liver biopsy showed diffuse swelling of cells in the liver lobules, cytoplasmic loosening from the cell wall, and spotty necrosis, but no piecemeal or bridging necrosis. Extensive lymphocyte infiltration in the portal area was observed, but no obvious fibrous tissue hyperplasia was detected (Figure 1).

Table 1
Laboratory results in the proband with autoimmune hepatitis and hereditary spherocytosis and her family members

	Proband	Paternal Grandmother	Father	Mother	Reference range
RBC ($\times 10^{12}$/L)	3.93	3.61	4.81	4.71	3.50–5.50
Hb (g/ L)	114.70	92.30	128.20	138.40	110.00–160.00
MCV (fL)	81.35	72.45	76.61	88.39	82.00–100.00
MCH (pg)	29.22	25.57	26.65	29.41	27.00–34.00
MCHC (g/L)	359.10	352.90	347.90	332.80	316.00–354.00
MSCV (f L)	60.29	60.80	62.80	84.08	84.00–104.00
MRV (f L)	73.04	80.95	80.50	99.05	101.00–119.00
RET (%)	10.30	7.00	4.40	1.00	0.00–2.00
TBIL (μmol/L)	64.30	43.60	26.70	8.50	3.40–20.50
DBIL (μmol/L)	32.00	3.80	2.80	2.50	0.00–6.80
IBIL (μmol/L)	32.30	39.80	23.90	6.00	3.10–14.30
ALT (U/L)	137	32	28	19	7–45
AST (U/L)	107	37	33	26	13–40
SF (ng/mL)	131.52	150.14	165.40	174.04	4.63-204.00
SI (μmol/L)	16.10	18.90	21.30	24.20	9.00-27.00
TIBC (μmol/L)	55.06	64.80	62.17	68.24	54.00-77.00
UIBC (μmol/L)	38.96	45.90	40.87	44.04	38.00-64.00
ISAT (%)	29.24	29.17	34.26	35.46	25.00-45.00

RBC, red blood cell count; Hb, hemoglobin; MCV, mean corpuscular volume; MCH, mean corpuscular hemoglobin; MCHC, mean corpuscular hemoglobin concentration; MSCV, mean sphered corpuscular volume; MRV, mean reticulocyte volume; RET, reticulocyte ratio; TBIL, total bilirubin; DBIL, direct bilirubin; IBIL, indirect bilirubin; ALT, alanine aminotransferase; AST, aspartate aminotransferase; SF, serum ferritin; SI, serum iron; TIBC, total iron binding capacity; UIBC, unsaturated iron binding capacity; ISAT, iron saturation.

2.2 Pedigree investigation

The marriage of the proband's parents was not consanguineous. Both her father and paternal grandmother had a history of splenomegaly and yellow sclerae. The mother had no clinical manifestations. We decided to perform further laboratory tests and HS gene mutation analysis on the

proband, her parents, and the paternal grandmother to further identify the etiology of impaired liver function.

2.3 Sample collection

The proband's parents provided written informed consent for all procedures associated with the study, and the Ethics Committee at the First Affiliated Hospital of Guangxi Medical University approved the study protocol. All procedures were conducted according to the principles expressed in the Declaration of Helsinki 1964 and its later amendments. Thereafter, we drew peripheral venous blood from the proband and her family members, using three tubes per person. Two tubes were used to collect EDTA-K2-anticoagulated whole blood. One of the two tubes was used for routine blood tests, reticulocyte detection, and peripheral red blood cell morphology examination. Red blood cell parameters were analyzed with a Coulter LH780 Hematology Analyzer (Beckman Coulter, Brea, CA, USA). The second tube was used for extracting genomic DNA from peripheral blood with a DNA Extraction Kit (Beijing Tiangen Biochemical Technology Co., Ltd., Beijing, China). The third tube contained separation gel for blood coagulation and was used for liver function tests performed with a 7600 Automatic Biochemical Analyzer (Hitachi Ltd., Tokyo, Japan).

2.4 Erythrocyte osmotic fragility test

The erythrocyte osmotic fragility test was carried out as described in previous studies[9]. Briefly, EDTA blood samples were added in series of saline solutions of increasingly saline concentration (0.0–0.9% w/v NaCl) and incubated at room temperature for 120 min. After centrifugation at 200 g for 5 min, the results were determined by naked eye visualization. Reddish-clear supernatant was seen in hemolysis positive tubes while colorless transparent supernatant was seen in negative tubes. The initial and complete hemolysis values of the proband and her family members were collected.

2.5 Next-generation sequencing

The extracted genomic DNA of the proband was sent to the Jinzhun Medical Laboratory (Beijing Jinzhun Gene Technology Co., Ltd., Beijing, China). Sequence variations of the whole exon coding regions and splicing regions of blood disease-related genes were analyzed by target region capture and high-throughput sequencing technology (Illumina HiSeq2500 System, Illumina, San Diego, CA, USA). Sequence alignment was performed using Burrows-Wheeler Aligner software. Mutations were identified using the Genome Analysis Toolkit (Broad Institute, Cambridge, MA, USA; https://gatk.broadinstitute.org/hc/en-us) and VarScan (Genome Institute, Washington University, Washington, WA, USA; http://varscan.sourceforge.net/) software, including the detection, annotation, and statistical analysis of single-nucleotide polymorphisms (SNP), InDels, etc. Information was obtained from an external database using ANNOVAR software (https://annovar.openbioinformatics.org/) to evaluate the effect of a given sequence mutation and list the mutations [10]. According to the sequencing analysis results, HS-related gene mutations were first considered, and the pathogenic mutations were found by referring to the dbSNP, 1000G, and EXAC databases.

2.6 Sanger sequencing

According to the results of next-generation sequencing, polymerase chain reaction (PCR)-Sanger sequencing was used to detect and verify mutations in the proband, her parents, and paternal grandmother. NM_003126 was used as the reference transcript of the *SPTA1* gene. The following primers were used for PCR: *SPTA1*c.134G>A (p.R45K) forward 5'-ACTTCCCACTCCACTGACT-3' and reverse 5'-TGACACATATAAGCGGGGCA-3'; and *SPTA1*c.6544G>C (p.D2182H) forward 5'-GCAATGTAGGCAAGATTCCGT-3' and reverse 5'-TCTCAGAGTGGGAGAGGCC-3'. PCR was performed using I-5™ 2× High-Fidelity Master Mix (MACLAB, San Francisco, CA, USA) in a 50 μL solution that included 21 μL water, 25 μL 2·Taq PCR Master Mix(Sangon Biotech Co., Ltd., Shanghai, China), 1 μL forward primer, 1 μL reverse primer, and 2 μL cDNA. PCR conditions included an initial denaturation at 95 ˚C for 5 min, followed by 35 cycles at 95 ˚C for 30 s, 60 ˚C for 30 s, 72 ˚C for 40 s, and a final extension at 72 ˚C for 8 min.

2.7 Pathogenicity prediction and analysis of gene mutation conservation

For the *SPTA1* gene c.134G>A (p.R45K) and c.6544G>C (p.D2182H) mutation sites, PolyPhen-2 (http://genetics.bwh.harvard.edu/pph2/index.shtml), Mutation Taster (http://www.mutationtaster.org/), SIFT (https://sift.bii.a-star.edu.sg/), and PROVEAN (http://provean.jcvi.org/index.php. J. Craig Venter Institute, La Jolla, CA, USA) software tools were used to evaluate their pathogenicity [11–13]. DNAMAN software (Lynnon Biosoft, San Ramon, CA, USA) was used to analyze the conservation of the *SPTA1* amino acid sequence among different species.

2.8 Protein structure analysis

HOPE software (https://www3.cmbi.umcn.nl/hope/) [14] was used to conduct homologous modeling of the *SPTA1* gene c.134G>A (p.R45K) and c.6544G>C (p.D2182H) mutation sites to predict the influence of amino acid residue changes caused by gene mutations affecting protein functions. The sequence relative to *SPTA1* was downloaded from UniProtKB (https://www.uniprot.org/uniprot/P02549).

3. Results

3.1 Laboratory results of the proband and her family members

Routine blood and reticulocyte test results of the proband and her family members showed that, except for the mother, all family members had increased RET and MSCV < MCV, MCV-MSCV > 9.6 fl, and MRV < 95.77 fl. Liver function tests showed that the proband's ALT, AST, TBIL, DBIL, and IBIL were all elevated. TBIL and IBIL values were elevated in the father and paternal grandmother, while DBIL, ALT, and AST values were normal. The mother’s liver function results were all normal. Serum ferritin and iron four test results of the proband and her family members were also normal (Table 1). Other laboratory test results of the proband in Table 2.

Table 2
Other laboratory test results of the proband

	Results	Reference range
IgG (g/L)	18.890	8.00–18.00
IgA (g/L)	0.840	0.90–4.50
IgM (g/L)	2.230	0.84–1.32
γ-globulin	26.00	11.10–18.80
ANA	±	-
SMA	+(Titer 1:320)	-
ANA karyotype	Homogeneous (1:100)	-
LKM-1	-	-
LC-1	-	-
AFP (ng/mL)	84.73	0.89–8.78
HBS Ag	0.00	0.00–0.50
HAV-IgM	-	-
HCV-Ab	-	-
HEV-Ab	-	-

-, negative; +, positive; ±,weak positive; Ig, immunoglobulin; ANA, antinuclear antibody; SMA, smooth muscle antibody; LKM-1, anti-liver and kidney microsomal antibody type 1; LC-1, antibody against liver cytosol type-1 antigen; AFP, alpha-fetoprotein; HBS Ag, hepatitis B surface antigen; HAV-IgM, hepatitis A IgM antibody; HCV-Ab, hepatitis C antibody; HEV-Ab, hepatitis E antibody.

Proband peripheral blood smears showed mature red blood cells that were slightly different in size, including mainly small cells, some cells with hyperpigmentation, and spherical cells that accounted for 18 % of the red blood cells. Spherical cells accounted for 13 % and 16 % of the red blood cells in the peripheral blood smears of the father and paternal grandmother, respectively. Peripheral blood smear results of the mother were normal (Figure 2).

3.2 Erythrocyte osmotic fragility test

The erythrocyte osmotic fragility test results showed that the initial (normal range: 4.2–4.6 g/L) and complete (normal range: 3.20–3.40 g/L) hemolysis values were, respectively, 6.0 and 5.30 g/L for the proband; 4.90 and 3.8 g/L for the proband's father; 5.10 and 4.2 g/L for the proband's paternal grandmother; 4.30 and 3.3 g/L for the proband's mother. Other laboratory findings for the proband and

her family members showed no abnormalities in the thalassemia gene test, normal G6PD activities, and negative Coombs tests.

3.3 Genetic test results for HS

Genetic testing showed that the spectrin alpha, erythrocytic 1 (*SPTA1*) gene of the proband had novel compound heterozygous mutations in exon 2 c.134G>A (p.R45K) and exon 46 c.6544G>C (p.D2182H). The *SPTA1* c.134G>A (p.R45K) mutation was inherited from the mother (Figure 3), whereas the *SPTA1* c.6544G>C (p.D2182H) mutation was inherited from the father; the paternal grandmother had the same mutation as the father (Figure 4).

3.4 Prediction of gene mutation pathogenicity and analysis of conservation

SPTA1 c.134G>A (p.R45K) is a novel missense mutation and was not found in the Human Gene Mutation Database. The ClinVar database does not include a pathogenicity analysis of this site; however, the mutation was predicted to be ‘benign’ in Polyphen-2 (score 0.052), ‘disease-causing’ in Mutation Taster (26), ‘tolerated’ in SIFT (0.478), and ‘neutral’ in PROVEAN.

SPTA1 c.6544G>C (p.D2182H) is also a novel missense mutation that was not found in the Human Gene Mutation Database. The ClinVar database does not include a pathogenicity analysis of this site. Polyphen-2 (score 0.990), Mutation Taster (81), SIFT (0.001), and PROVEAN (-3.09) predicted a pathogenic effect describing it as ‘probably damaging’, ‘disease-causing’, ‘damaging’, and ‘deleterious’, respectively. Conservative sequence analysis showed that the c.134G>A (p.R45K) and c.6544G>C (p.D2182H) sites of the *SPTA1* gene are highly conserved among different species (Figure 5). The p.R45K and p.D2182H variants are classified as a variant of uncertain significance (VUS) by the American College of Medical Genetics and Genomics (ACMG) criteria.

3.5 Protein structure analysis of the SPTA1 c.134G>A mutation

Protein structure analysis of the *SPTA1* c.134G>A (p.R45K) mutation showed that the mutant residue is smaller than the wild-type residue, and that the wild-type residue forms a hydrogen bond with aspartic acid at position 291. The size difference means that the mutant residue is not in the correct position to form the same hydrogen bond as the original wild-type residue (Figure 6). Schematics for c.6544G>C (p.D2182H) could not be generated as the 3D structures were unavailable in the HOPE database [14].

4. Discussion

AIH is an inflammation of the liver parenchyma caused by an autoimmune response to hepatocytes. It is characterized by elevated transaminase serum levels, positive serum autoantibodies, high IgG and/or γ-globulinemia, and interstitial hepatitis upon histological examination [1]. According to the pattern of autoantibodies detected, a subclassification into three disease subtypes has been proposed: AIH-1, AIH-2,

and AIH-3. AIH-1 is characterized by the presence of ANA and/or SMA. AIH-2 is characterized by the specific anti-liver and kidney microsomal antibody type-1, infrequently anti-LKM type-3, and/or antibody against liver cytosol type-1 antigen. AIH-3 is characterized by soluble liver antigen/liver pancreas antibodies [15]. The clinical manifestations of AIH are diverse, but most patients have an insidious onset, presenting as chronic liver disease [16]. The most common symptoms include lethargy, fatigue, and intermittent jaundice, while physical examination may reveal hepatomegaly, splenomegaly, ascites, and, occasionally, peripheral edema [1, 17]. In our study, the patient presented with yellow sclerae; liver and spleen enlargement; elevated levels of ALT, AST, TBIL, IBIL, and DBIL; positive ANA and SMA; slightly increased IgG; and increased γ-globulin levels. Her liver biopsy showed diffuse swelling of the liver lobule cells, cytoplasmic loosening, spotty necrosis, and extensive lymphocyte infiltration in the portal area. Based on these findings, the patient was diagnosed with AIH. In addition, morphological examination of her peripheral red blood cells showed that 18 % were spherical; the MCV, MSCV, and MRV were decreased; RET was increased; G-6-PD activity was normal; and the Coombs test was negative. These findings indicated that the patient's abnormal liver function did not result from AIH alone, but that she might also suffer from hemolytic anemia.

HS is a common hereditary hemolytic disease. Gene mutations lead to defects in erythrocyte membrane proteins, which weaken the vertical connection between the protein and lipid bilayer[18]. This results in destabilization or loss of the membrane lipid bilayer and the formation of microvesicles, reducing the cell membrane surface area to volume ratio and changing the red blood cell morphology from a biconcave disc to a spherical shape. These changes reduce the deformability and increase the osmotic fragility of erythrocytes, resulting in their destruction when passing through the small splenic vessels and, ultimately, hemolytic anemia. Clinical manifestations vary widely among HS patients. Those with severe and moderate HS often have anemia, jaundice, and splenomegaly, whereas patients with mild HS have either atypical symptoms or are asymptomatic [4]. The guidelines for the diagnosis and treatment of HS, developed by the British Committee for Standards in Hematology [6], recommend that patients who have a positive family history, typical clinical features, and increased MCHC, spherocytosis, and reticulocytes, compared to normal values, should be diagnosed with HS without further examination. Therefore, patients with mild HS and no symptoms are easily misdiagnosed, or the diagnosis is entirely missed. Furthermore, because of the similar clinical manifestations of HS and AIH, such as jaundice and splenomegaly, the diagnosis of HS is frequently missed even in symptomatic patients and misdiagnosed as AIH. Deng et al. [19] reported a patient with mild HS who had jaundice but no symptoms of anemia and was misdiagnosed with AIH. The type of jaundice can be classified by measuring TBIL, DBIL, and IBIL. Patients with hepatobiliary disorders frequently have increased TBIL, mainly attributable to an increase in DBIL. Patients with hemolytic anemia also have increased TBIL, but it is mainly attributable to an increase in IBIL. In our patient, TBIL was increased due to both DBIL and IBIL, each accounting for 50 %. The patient had hepatomegaly and splenomegaly but no anemia symptoms, which might have easily led to missing the diagnosis of HS.

Erythrocyte morphology, blood count, and assessment of reticulocyte-related variables are simple, rapid, and practical means of diagnosing HS, which can be assessed in routine laboratories. When spherocytes

comprised more than 7.8 % of red blood cells, the sensitivity and specificity for diagnosing HS were 56.7 % and 84.8 %, respectively [20]. Spherocytes are also present in peripheral blood smears of patients with G6PD deficiency and autoimmune hemolytic anemia [5]. Liao et al. [21] reported that when using an MCHC ≥ 334.9 g/L as the threshold, the HS diagnosis sensitivity was 82.1 %, and the specificity was 94.5 %. An increase in serum bilirubin can induce a false increase in MCHC. MSCV is a specific spherocyte measure and, in combination with MCV, can be highly effective in diagnosing HS. For example, Chiron et al. [22] reported that when the MSCV < MCV, the sensitivity and specificity for diagnosing HS were 100 % and 93.3 %, respectively. Broséus et al. [23] found that when the Coombs test was negative and the MCV-MSCV was > 9.6 fl, the sensitivity and specificity for diagnosing HS were 100 % and 90.57 %, respectively. In turn, Xu et al. [24] reported that the MRV is ideal for diagnosing HS; when the MRV was ≤ 95.77 fl, sensitivity and specificity were 86.80 % and 91.20 %, respectively. Our patient met all these diagnostic criteria. Thus, her laboratory results were highly suggestive of HS, but she had no typical clinical symptoms or positive family history. As a consequence, genetic analysis became necessary for an accurate diagnosis.

Through high-throughput sequencing, we found two novel compound heterozygous mutations, one in exon 2 c.134G>A (p.R45K) and one in exon 46 c.6544G>C (p.D2182H) of the *SPTA1* gene. PCR combined with Sanger sequencing confirmed that the first mutation was from the asymptomatic mother, and the second mutation was from the father, who had a history of splenomegaly and yellow sclerae. The mother's laboratory test results were normal, whereas her father and paternal grandmother showed an similar clinical and blood analysis results to the proband. Therefore, we hypothesized that the heterozygous mutation c.134G>A (p.R45K) inherited from the mother was more likely to be benign, and the heterozygous missense mutation c.6544G>C (p.D2182H) inherited from the father was more likely to be pathogenic.

The 80 Kb *SPTA1* gene is located in the q22-q23 region of chromosome 1. It contains 52 exons and encodes α-spectrin, which contains 2419 amino acids. α-spectrin is a cytoskeletal protein that combines with β-spectrin to form α-β heterodimers in a reverse parallel arrangement. The terminal end of the polymers formed by the two heterodimers combine with actin and transmembrane proteins forming a "junction complex." The latter forms a grid structure in the cell membrane, maintaining lipid bilayers and the biconcave disc shape of the erythrocytes [25]. The expression of α-spectrin is four times that of β-spectrin, and the formation of α-β heterodimers is not affected by relative decreases in α-spectrin expression [26]. Therefore, homozygous or compound heterozygous mutations in the *SPTA1* gene may be involved in the pathogenesis of HS with recessive α-spectrin deficiency; heterozygous individuals may still produce enough α-spectrin to balance β-spectrin production and maintain the erythrocyte cytoskeleton [27, 28]. The *SPTA1* missense mutation of c.134G>A (p.R45K) resulted in the 45th amino acid being changed from arginine to lysine. Amino acid sequence analysis showed that the mutation site is highly conserved among different species. In the protein structure analysis, the mutant residue was smaller than the wild-type residue, and the wild-type residue was found to be involved in a multimer contact. It is possible that the mutant residue is too small to make multimer contacts and thereby negatively affects the function of α-spectrin. The missense mutation of c.6544G>C (p.D2182H) resulted

in the 2182nd amino acid being changed from aspartic acid to histidine. This site is also highly conserved among different species. Protein structure analysis revealed that this mutation is located within a repeated stretch of residues in the protein, called spectrin 20. The mutation into another residue might disturb this repeat and consequently any related function. The mutated residue is located in a domain that is important for the binding of other molecules and thus, may disturb this function [14]. Furthermore, the c.6544G>C (p.D2182H) mutation was predicted to have a pathogenic effect by Polyphen-2, Mutation Taster, SIFT, and PROVEAN. Therefore, the novel compound heterozygous mutations c.134G>A (p.R45K) and c.6544G>C (p.D2182H) in the *SPTA1* gene might have caused HS in this patient with AIH.

5. Conclusion

Patients who have both HS and AIH are very rare. HS has clinical manifestations similar to AIH, making it difficult to diagnose HS when it coexists with AIH. When laboratory results cannot be explained by autoimmune liver disease alone, the possibility of another concomitant disease should be considered; pedigree investigation and genetic analyses may be required for the final diagnosis.

Declarations

Ethics approval and consent to participate:

Including a statement on ethics approval and consent; Including the name of the ethics committee that approved the study and the committee's reference number (2021(KY-E-078)); Including a statement on informed consent from the patient's famaly.

Consent for publication:

The proband's parents provided written informed consent for all procedures associated with the study, and the Ethics Committee at the First Affiliated Hospital of Guangxi Medical University approved the study protocol.

Availability of data and materials:

The datasets used and/or analysed during the current study are available from the corresponding author on reasonable request.

Competing interests:

The authors declare that they have no conflict of interest with the content of this article.

Funding:

This study was supported by the National Natural Science Foundation of China (no. 81360263).

Authors' contributions:

Yu-mei Qin and Yan-yun Chen researched literature and conceived the study. Lin Liao ,Yang-yang Wu , Min Chen and Fa-quan Lin were involved in protocol development, gaining ethical approval, patient recruitment and data analysis. Yu-mei Qin wrote the first draft of the manuscript. All authors reviewed and edited the manuscript and approved the final version of the manuscript.

Acknowledgements:

We would like to thank the patient and her family for their cooperation.

References

1. Floreani A, Restrepo-Jimenez P, Secchi MF, De Martin S, Leung PSC, Krawitt E, et al. Etiopathogenesis of autoimmune hepatitis. J Autoimmun. 2018;95:133-143.
2. Puustinen L, Barner-Rasmussen N, Pukkala E, Farkkila M. Incidence, prevalence, and causes of death of patients with autoimmune hepatitis: A nationwide register-based cohort study in Finland. Dig Liver Dis. 2019;51(9):1294-1299.
3. Tunio NA, Mansoor E, Sheriff MZ, Cooper GS, Sclair SN, Cohen SM. Epidemiology of Autoimmune Hepatitis (AIH) in the United States Between 2014 and 2019: A Population-based National Study. J Clin Gastroenterol. 2020.
4. Manciu S, Matei E, Trandafir B. Hereditary Spherocytosis - Diagnosis, Surgical Treatment and Outcomes. A Literature Review. Chirurgia (Bucur). 2017;112(2):110-116.
5. King MJ, Garcon L, Hoyer JD, Iolascon A, Picard V, Stewart G, et al. ICSH guidelines for the laboratory diagnosis of nonimmune hereditary red cell membrane disorders. Int J Lab Hematol. 2015;37(3):304-325.
6. Bolton-Maggs PH, Langer JC, Iolascon A, Tittensor P, King MJ, General Haematology Task Force of the British Committee for Standards in H. Guidelines for the diagnosis and management of hereditary spherocytosis–2011 update. Br J Haematol. 2012;156(1):37-49.
7. Wang C, Cui Y, Li Y, Liu X, Han J. A systematic review of hereditary spherocytosis reported in Chinese biomedical journals from 1978 to 2013 and estimation of the prevalence of the disease using a disease model. Intractable Rare Dis Res. 2015;4(2):76-81.
8. Narla J, Mohandas N. Red cell membrane disorders. Int J Lab Hematol. 2017;39 Suppl 1:47-52.
9. Huisjes R, Makhro A, Llaudet-Planas E, Hertz L, Petkova-Kirova P, Verhagen LP, et al. Density, heterogeneity and deformability of red cells as markers of clinical severity in hereditary spherocytosis. Haematologica. 2020;105(2):338-347.
10. Wang K, Li M, Hakonarson H. ANNOVAR: functional annotation of genetic variants from high-throughput sequencing data. Nucleic Acids Res. 2010;38(16):e164.

11. Adzhubei I, Jordan DM, Sunyaev SR. Predicting functional effect of human missense mutations using PolyPhen-2. Curr Protoc Hum Genet. 2013;Chapter 7:Unit7.20.
12. Schwarz JM, Cooper DN, Schuelke M, Seelow D. MutationTaster2: mutation prediction for the deep-sequencing age. Nat Methods. 2014;11(4):361-362.
13. Vaser R, Adusumalli S, Leng SN, Sikic M, Ng PC. SIFT missense predictions for genomes. Nat Protoc. 2016;11(1):1-9.
14. Venselaar H, Te Beek TA, Kuipers RK, Hekkelman ML, Vriend G. Protein structure analysis of mutations causing inheritable diseases. An e-Science approach with life scientist friendly interfaces. BMC Bioinformatics. 2010;11:548.
15. European Association for the Study of the L. EASL Clinical Practice Guidelines: Autoimmune hepatitis. J Hepatol. 2015;63(4):971-1004.
16. Porta G, Carvalho Ed, Santos JL, Gama J, Borges CV, Seixas RBPM, et al. Autoimmune hepatitis in 828 Brazilian children and adolescents: clinical and laboratory findings, histological profile, treatments, and outcomes. Jornal de Pediatria (Versão em Português). 2019;95(4):419-427.
17. Sucher E, Sucher R, Gradistanac T, Brandacher G, Schneeberger S, Berg T. Autoimmune Hepatitis-Immunologically Triggered Liver Pathogenesis-Diagnostic and Therapeutic Strategies. J Immunol Res. 2019;2019:9437043.
18. Donato H, Crisp RL, Rapetti MC, García E, Attie M. [Hereditary spherocytosis: Review. Part I. History, demographics, pathogenesis, and diagnosis]. Arch Argent Pediatr. 2015;113(1):69-80.
19. Deng Z, Liao L, Yang W, Lin F. Misdiagnosis of two cases of hereditary spherocytosis in a family and review of published reports. Clin Chim Acta. 2015;441:6-9.
20. Mullier F, Lainey E, Fenneteau O, Da Costa L, Schillinger F, Bailly N, et al. Additional erythrocytic and reticulocytic parameters helpful for diagnosis of hereditary spherocytosis: results of a multicentre study. Ann Hematol. 2011;90(7):759-768.
21. Liao L, Xu Y, Wei H, Qiu Y, Chen W, Huang J, et al. Blood cell parameters for screening and diagnosis of hereditary spherocytosis. J Clin Lab Anal. 2019;33(4):e22844.
22. Chiron M, Cynober T, Mielot F, Tchernia G, Croisille L. The GEN.S: a fortuitous finding of a routine screening test for hereditary spherocytosis. Hematology & Cell Therapy. 1999;41(3):113-116.
23. Broseus J, Visomblain B, Guy J, Maynadie M, Girodon F. Evaluation of mean sphered corpuscular volume for predicting hereditary spherocytosis. Int J Lab Hematol. 2010;32(5):519-523.
24. Xu Y, Yang W, Liao L, Deng Z, Qiu Y, Chen W, et al. Mean reticulocyte volume: a specific parameter to screen for hereditary spherocytosis. Eur J Haematol. 2016;96(2):170-174.
25. He BJ, Liao L, Deng ZF, Tao YF, Xu YC, Lin FQ. Molecular Genetic Mechanisms of Hereditary Spherocytosis: Current Perspectives. Acta Haematol. 2018;139(1):60-66.
26. Eber S, Lux SE. Hereditary spherocytosis--defects in proteins that connect the membrane skeleton to the lipid bilayer. Semin Hematol. 2004;41(2):118-141.

27. Nussenzveig RH, Christensen RD, Prchal JT, Yaish HM, Agarwal AM. Novel α-spectrin mutation in trans with α-spectrin causing severe neonatal jaundice from hereditary spherocytosis. Neonatology. 2014;106(4):355-357.
28. Chen M, Ye Y-P, Liao L, Deng X-L, Qiu Y-L, Lin F-Q. Hereditary spherocytosis overlooked for 7 years in a pediatric patient with β-thalassemia trait and novel compound heterozygous mutations of SPTA1 gene. Hematology. 2020;25(1):438-445.

Figures

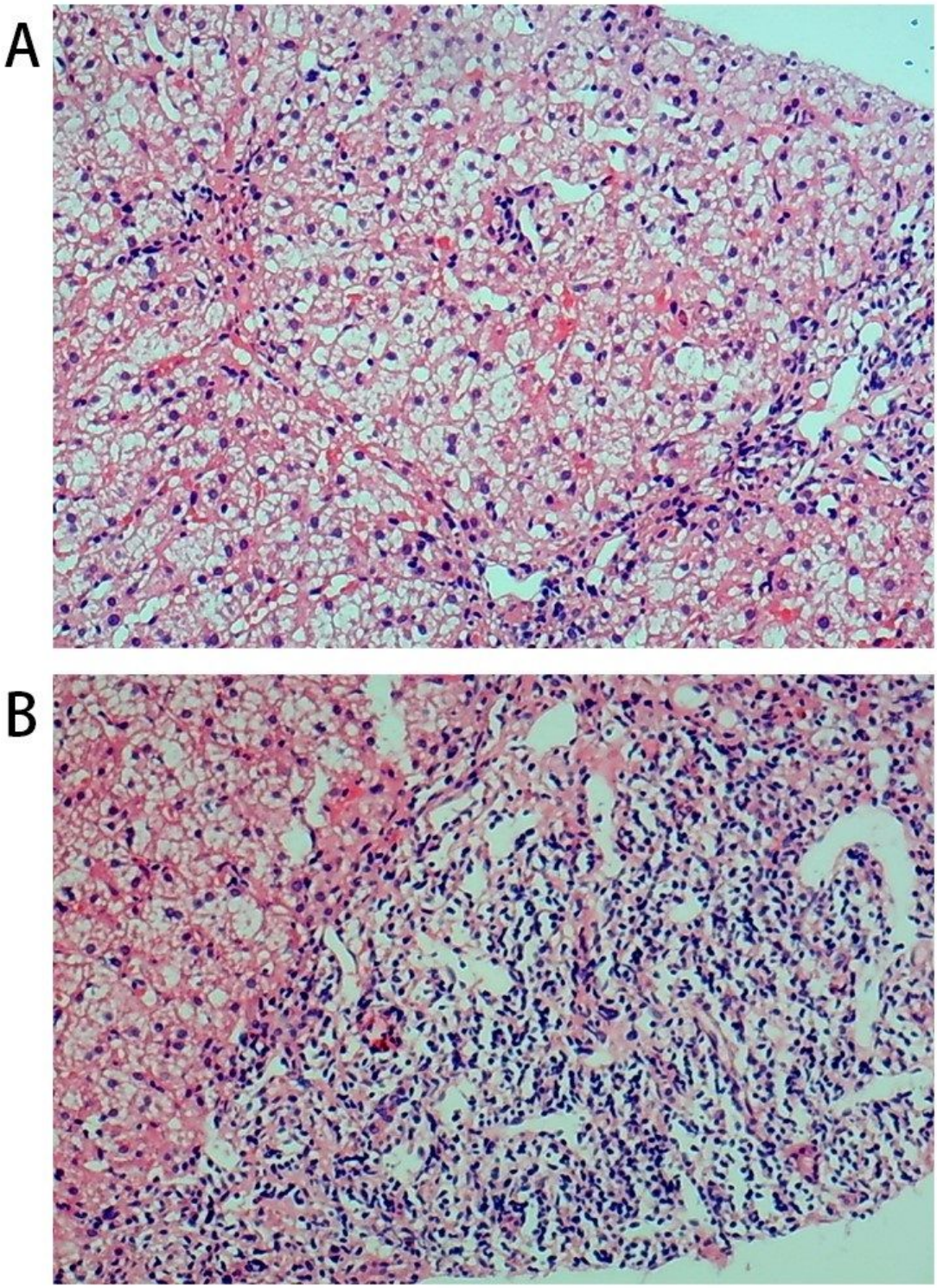

Figure 1

Histological investigation of the liver biopsy in a pediatric patient with autoimmune hepatitis and hereditary spherocytosis (hematoxylin-eosin staining, ×100). (A) Diffuse swelling of liver cells in the liver lobule and cytoplasmic loosening are visible. (B) Extensive lymphocyte infiltration in the portal area.

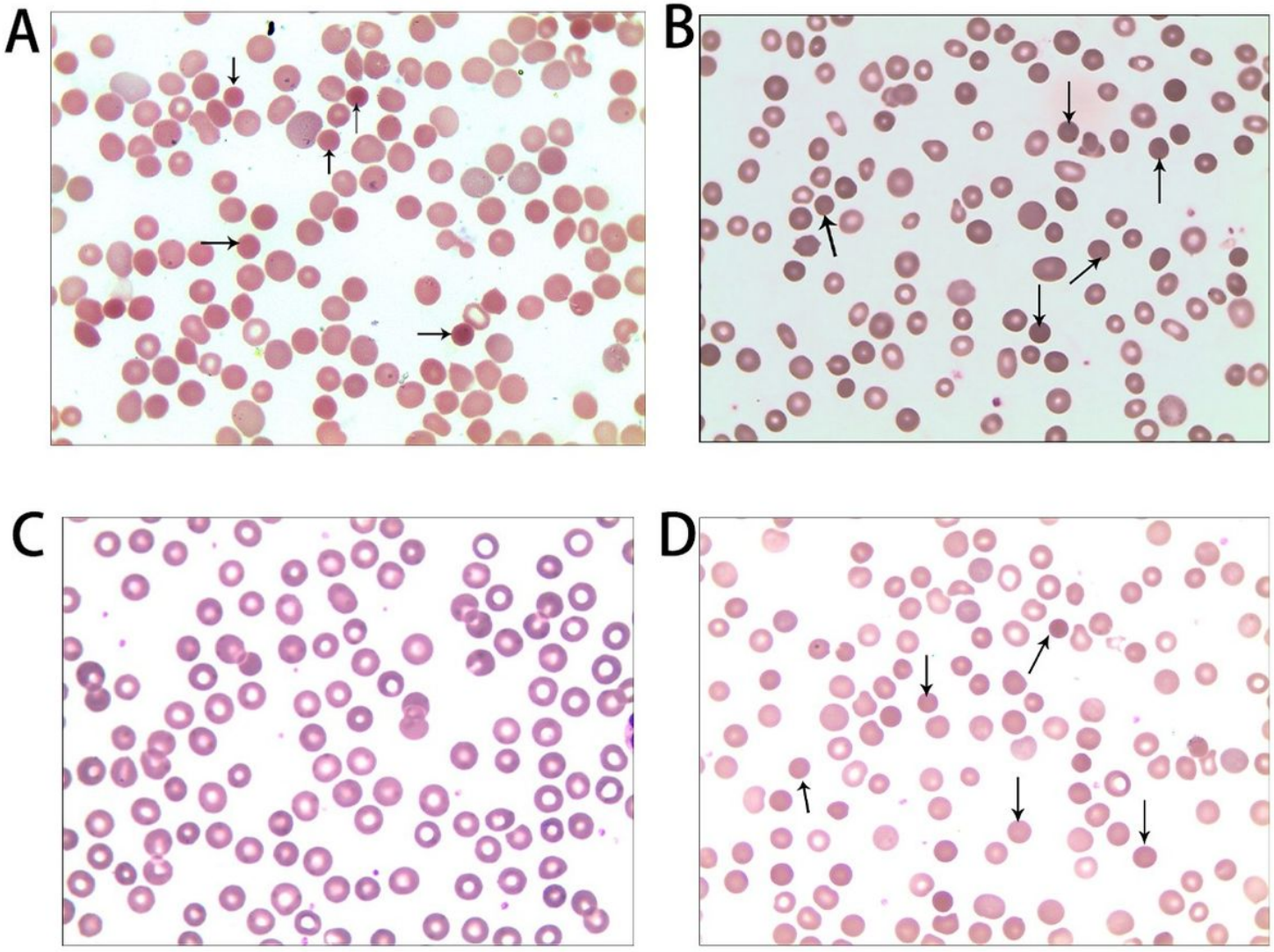

Figure 2

Morphology of peripheral blood erythrocytes (Wright–Giemsa, magnification, ×400). (A) Proband; (B) Father; (C) Mother; (D) Grandmother. The arrows show spherical red blood cells that are typical for hereditary spherocytosis.

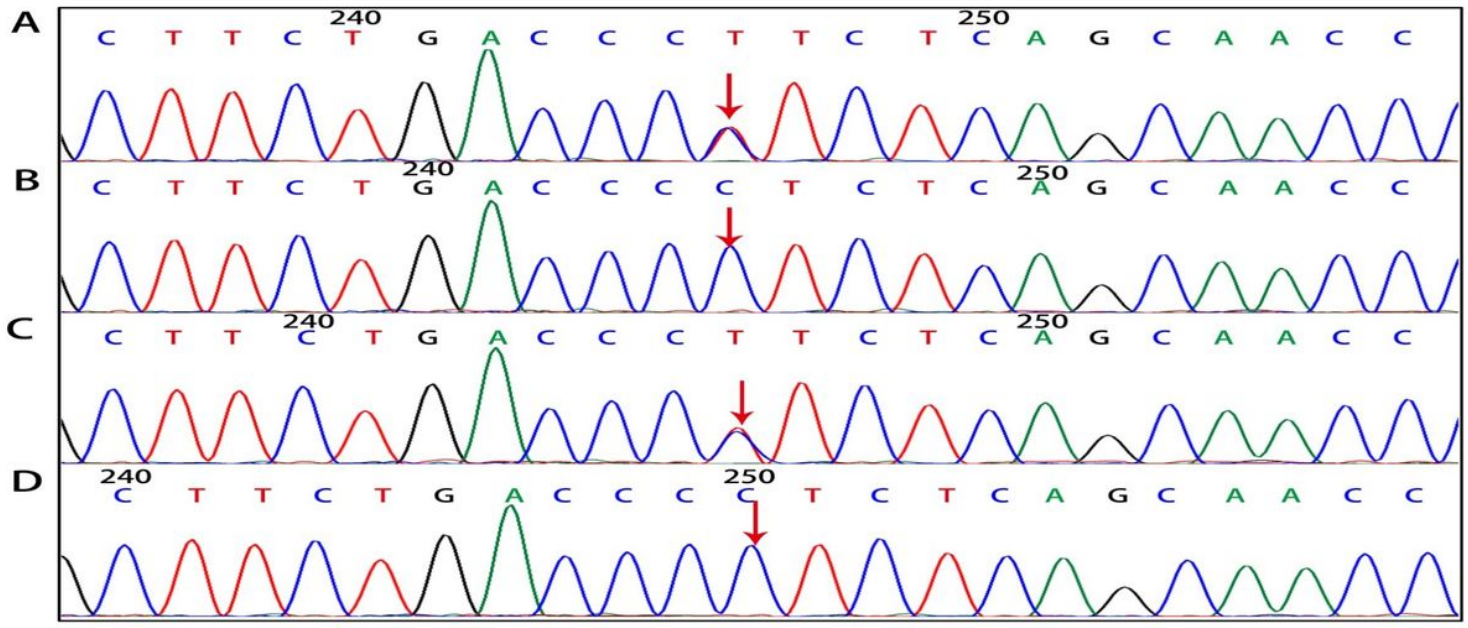

Figure 3

Findings of the SPTA1 gene c.134G>A (p.R45K) mutation. (A) Proband, heterozygous mutation; (B) Father, normal; (C) Mother, heterozygous mutation; (D) Grandmother, normal. The arrows in figure A and C indicate the mutation sites, while the arrows in figure B and D show that there is no mutation.

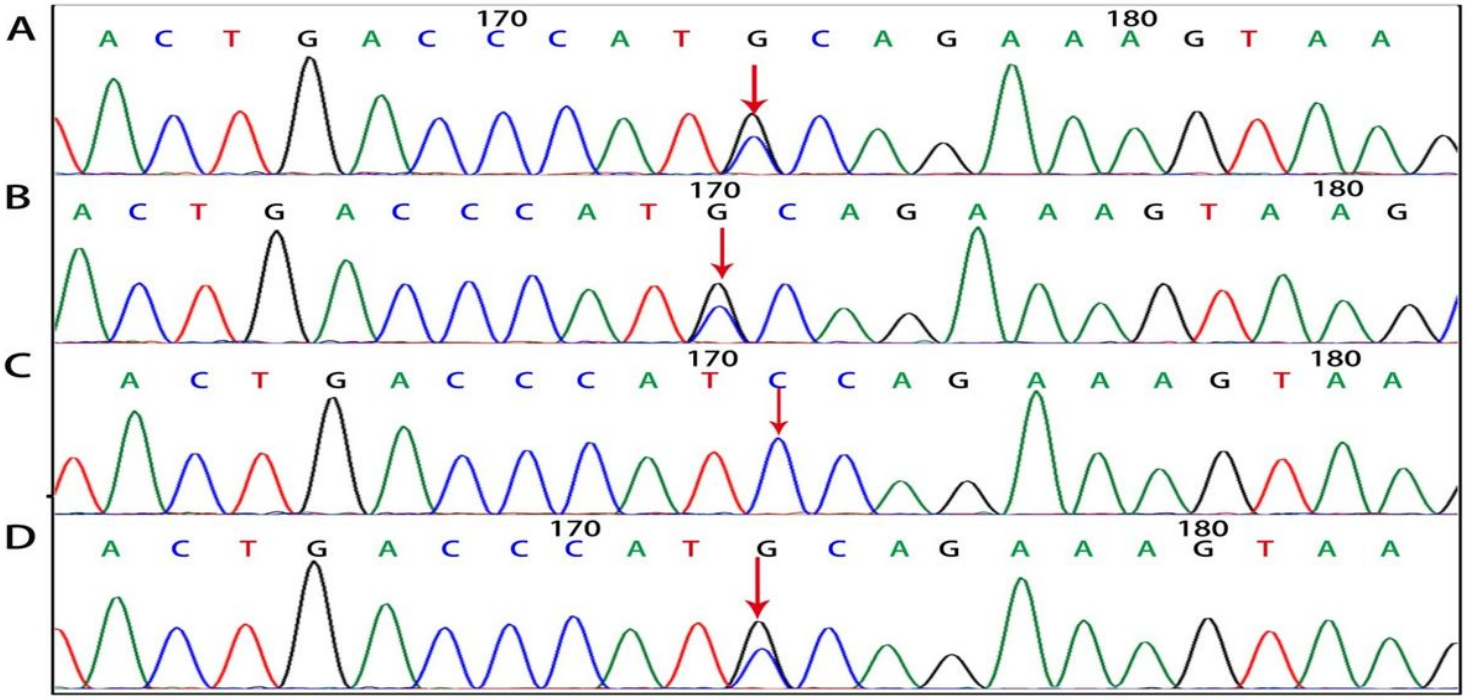

Figure 4

Findings of the SPTA1 gene c.6544G>C (p.D2182H) mutation. (A) Proband, heterozygous mutation; (B) Father, heterozygous mutation; (C) Mother, normal; (D) Grandmother, heterozygous mutation. The arrows

in figure A, B, and D indicate the mutation sites, while the arrows in figure C show that there is no mutation.

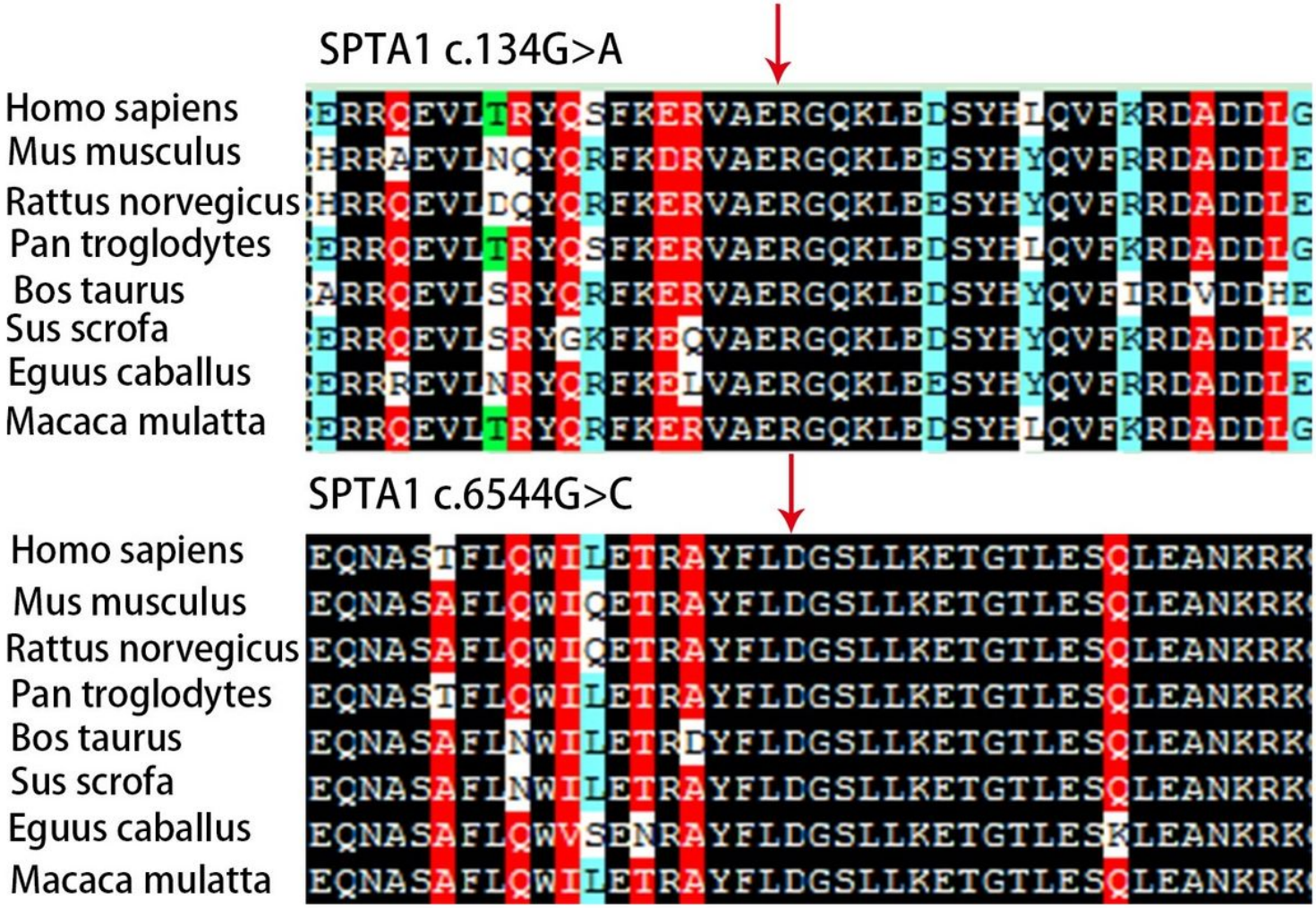

Figure 5

Conservation analysis of the c.134G> A (p.R45K) and c.6544G>C (p.D2182H) sequences of the SPTA1 gene among different species. The red arrow indicates that the mutation is located at a highly conserved amino acid site.

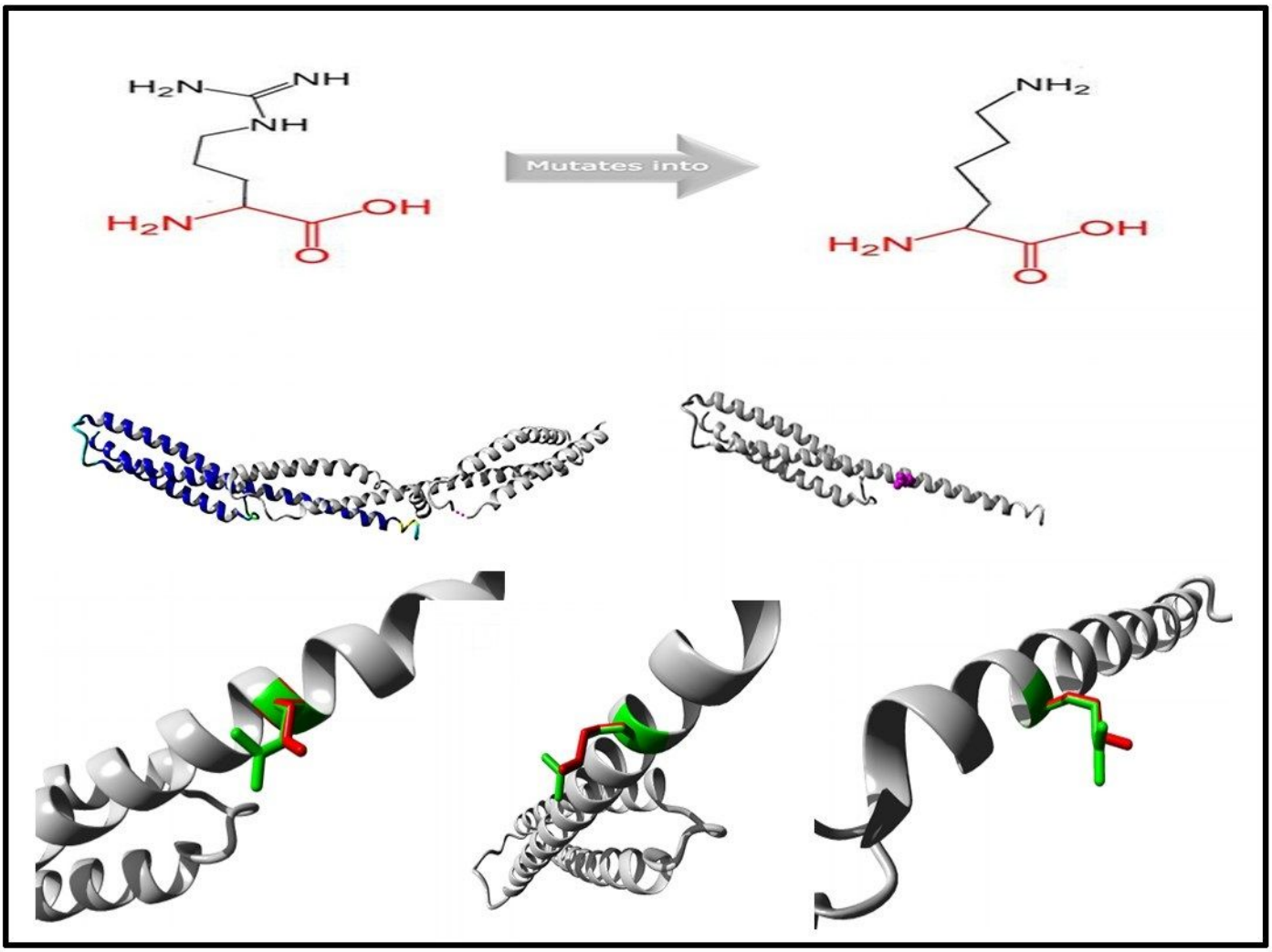

Figure 6

Protein structure analysis of SPTA1 c.134G>A (p.R45K). (A) The schematic structures of the original (left) and the mutant (right) amino acid. The backbone, which is the same for each amino acid, is colored in red. The side chain, unique for each amino acid, is colored in black. (B) On the left is an overview of the protein in ribbon-presentation. The protein is colored by element: α-helix = blue; β-strand = red; turn = green; 3/10 helix=yellow and random coil = cyan. Other molecules in the complex are colored grey when present. On the right is an overview of the mutant protein in ribbon-presentation. The protein is colored grey, the side chain of the mutated residue is colored magenta and shown as small balls. (C) The three different angles of the mutant structure are shown. The protein is gray, and the side chains of wild-type residues and mutant residues are green and red, respectively.